Electronic Supplementary Material (ESI) for CrystEngComm.
This journal is © The Royal Society of Chemistry 2022

Supporting Information

# Double Butterfly-shaped Octanuclear Dysprosium Cluster: Structure, Magnetism and Assembly Mechanism

Yun-Lan Li,[a] Zhong-Ming Huang,[a] Hai-Ling Wang,[a] Zhong-Hong Zhu,[a,*] Fu-Pei Liang,[a] and Hua-Hong Zou[a,*]

[a]School of Chemistry and Pharmaceutical Sciences, State Key Laboratory for Chemistry and Molecular Engineering of Medicinal Resources, Guangxi Normal University, Guilin 541004, P. R. China

*E-mail (Corresponding author): 18317725515@163.com (Z.-H. Zhu), gxnuchem@foxmail.com (H.-H. Zou).

## Table of Contents:

**Experimental Section**

**Materials and Measurements.**

All reagents were obtained from commercial sources and used without further purification. Elemental analyses for C, N, and H were performed on a varia MICRO cube. Infrared spectra were recorded by transmission through KBr pellets containing *ca.* 0.5% of the complexes using a PE Spectrum FT-IR spectrometer (400–4,000 $cm^{-1}$) (Figure S1). Thermogravimetric analyses (TGA) were conducted in a flow of nitrogen at a heating rate of 5 °C/min using a NETZSCH TG 209 F3 (Figure S2). Powder X-ray diffraction (PXRD) spectra were recorded on a D8 Advance (Bruker) diffractometer at 293 K (Mo-Kα). The samples were prepared by crushing crystals and the powder placed on a grooved aluminum plate. Diffraction patterns were recorded from 5º to 55º at a rate of 5º $min^{-1}$ (Figure S3). Measurements of magnetic susceptibility were carried out within the temperature range of 2–300 K using a Quantum Design MPMS SQUID magnetometer equipped with a 7 T magnet. The diamagnetic corrections for these complexes were estimated using Pascal's constants, and magnetic data were corrected for diamagnetic contributions of the sample holder.

**Single-crystal X-ray crystallography.**

Diffraction data for the complex were collected on a Bruker SMART CCD diffractometer (Cu-Kα radiation and $\lambda$ = 1.54 Å) in $\Phi$ and $\omega$ scan modes. The structures were solved by direct methods, followed by difference Fourier syntheses, and then refined by full-matrix least-squares techniques on $F^2$ using *SHELXL*[1]. All other non-hydrogen atoms were refined with anisotropic thermal parameters. Hydrogen atoms were placed at calculated positions and isotopically refined using a riding model. Table S1 summarizes X-ray crystallographic data and refinement details for the complexes. The CCDC reference numbers are 2217384 and 2217385 for **1** and **2**.

[1] Sheldrick, G. M. *Acta Crystallogr., Sect. C: Struct. Chem*. **2015**, *71*, 3-8.

**Reagents and Medicines**

All reagents used in this experiment were of AR grade without further purification. All reagents used include: anhydrous methanol (500 mL, AR), acetonitrile (500 mL, AR), triethylamine (500 mL, AR), $Dy(NO_3)_3·6H_2O$ (100 g, AR), 4-(dimethylamino)-2-hydroxybenzaldehyde (25 g, AR), 4-diethylaminosalicylaldehyde (25 g, AR), salicylic hydrazide (50 g, AR).

**The synthesis method.**

**Synthesis of cluster 1** ($[Dy_8(L^1)_4(\mu_3\text{-}O)_2(CH_3O)_6(NO_3)_4(CH_3OH)_6(H_2O)_2]·3CH_3OH·CH_3CN·H_2O$): Add 0.1 mmol (0.0165 g) 4-(dimethylamino)-2-hydroxybenzaldehyde, 0.1 mmol salicylic hydrazide (0.0152 g), 0.2 mmol (0.091 g) $Dy(NO_3)_3·6H_2O$, 60 μL triethylamine and 2.5 mL mixed solutions ($CH_3OH$ : $CH_3CN$ = 2 : 0.5) were added in a pyrex tube. In the tube, shake and sonicate for 15 min. Place the sealed pyrex tube in an oven at 80 ˚C, take it out two days later, slowly cool to room temperature, and precipitate brown lumpy crystals. The yield is about 31.5% (calculated with the amount of $Dy(NO_3)_3·6H_2O$). Elemental analysis theoretical value ($C_{78}H_{134}Dy_8O_{20}N_{46}$): C, 28.08%; H, 4.09%; N, 19.31%; experimental value: C, 28.01%; H, 4.03%; N, 19.28%. Infrared spectrum data (IR, KBr pellet, $cm^{-1}$): 3414(m), 2972(w), 2425(w), 1600(s), 1383(s), 1253(s), 1140(w), 1071(w), 837(w), 758(w), 489(m).

**Synthesis of cluster 2** ($[Dy_8(L^2)_4(\mu_3\text{-}O)_2(CH_3O)_6(NO_3)_4(CH_3OH)_6(H_2O)_2]·6CH_3OH·CH_3CN·H_2O$): The procedure was similar to that of cluster **1**, except that the 4-(dimethylamino)-2-hydroxybenzaldehyde was replaced with 4-diethylaminosalicylaldehyde. The yield is about 29% (calculated with the amount of $Dy(NO_3)_3·6H_2O$). Elemental analysis theoretical value ($C_{96}H_{170}Dy_8N_{18}O_{52}$): C, 31.09%; H, 4.62%; N, 6.79%; experimental value: C, 31.02%; H, 4.59%; N, 6.75%. Infrared spectrum data (IR, KBr pellet, $cm^{-1}$): 3403(m), 2423(w), 1599(s), 1512(m), 1382(s), 1251(m), 1138(w), 1060(w), 835(w), 756(w), 487(m).

**TableS1.**Crystallographic data of clusters **1** and **2**.

| | **1** | **2** |
|---|---|---|
| Formula | $C_{78}H_{134}Dy_8O_{20}N_{46}$ | $C_{96}H_{170}Dy_8N_{18}O_{52}$ |
| Formula weight | 3388.04 | 3648.75 |
| *T*, K | 100(10) | 100(10) |
| Crystal system | triclinic | triclinic |
| Space group | $P\bar{1}$ | $P\bar{1}$ |
| *a*, Å | 10.7519(2) | 14.1647(4) |
| *b*, Å | 15.0363(2) | 14.3993(3) |
| *c*, Å | 17.3580(3) | 16.7338(4) |
| *α*, ° | 71.4304(13) | 82.531(2) |
| *β*, ° | 81.7596(16) | 75.286(3) |
| *γ*, ° | 84.3800(14) | 82.046(2) |
| *V*, Å$^3$ | 2628.60 (8) | 3253.05(14) |
| *Z* | 1 | 1 |
| $D_c$, gcm$^{-3}$ | 2.140 | 1.863 |
| *μ*, mm$^{-1}$ | 30.67 | 24.87 |
| *F*(000) | 1638 | 1780 |
| 2*ϑ* range for data collection/° | 6.2 to 149.8 | 5.4 to 151 |
| Reflns coll. | 33758 | 39484 |
| Unique reflns | 10572 | 13042 |
| $R_{int}$ | 0.077 | 0.0575 |
| Observed data [*I*>2σ(*I*)] | 9170 | 11961 |
| $N_{par}$, $N_{ref}$ | 718, 10572 | 807, 3166 |
| $R_1$[a] (*I*>2σ(*I*)) | 0.086 | 0.1024 |
| $wR_2$[b] (all data) | 0.233 | 0.2811 |
| GOF | 1.03 | 1.10 |

[a]$R_1 = \Sigma||F_o|-|F_c||/\Sigma|F_o|$, [b]$wR_2 = [\Sigma w(F_o^2-F_c^2)^2/\Sigma w(F_o^2)^2]^{1/2}$

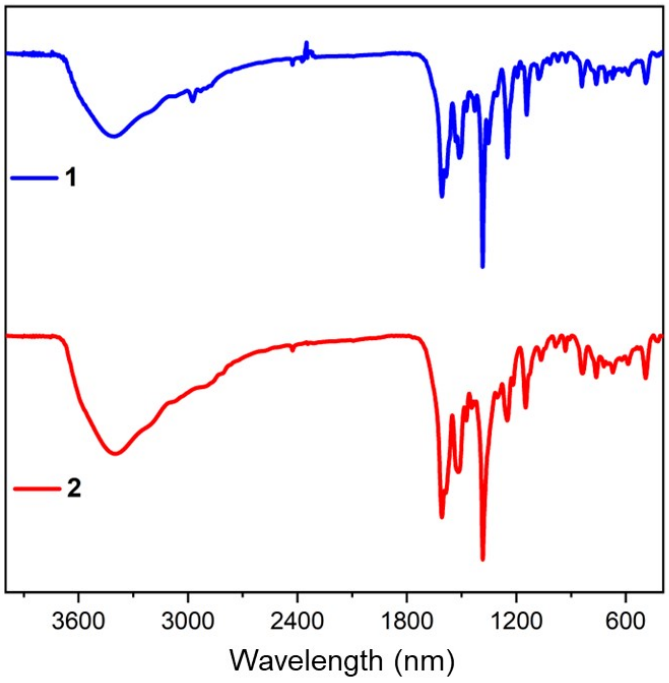


**Figure S1.** IR spectra of clusters **1** and **2**.

**Thermal analysis**

The thermal stability tests of clusters **1** and **2** were carried out under a flowing nitrogen atmosphere, and the temperature was slowly increased from 35 °C to 1000 °C at a rate of 5 °C/min. The structures of clusters **1** and **2** are similar, so the thermal stability test results are basically the same. First, when the temperature is gradually increased from 35 °C to 78 °C, the weight loss is 4.42%. This process corresponds to a loss of three $CH_3OH$ molecules, one $CH_3CN$ molecule and one $H_2O$ molecules (theoretical value is 4.57%). When the temperature continues to rise 195 °C, the weight loss is 2.32%. This process corresponds to a loss of two $CH_3OH$ molecules and one $H_2O$ molecule (theoretical value is 2.43%). Finally, the weight loss is 7.81%, when the temperature continues to rise from 195 °C to 350 °C. This process corresponds to a loss of four $CH_3OH$ molecules and two $NO_3^-$ ions (theoretical value is 7.91%). When the temperature continues to rise above 350 °C, cluster **1** was decomposed as the temperature continued to rise (Figure S2a). Cluster **2** has a weight loss of 4.98% before 152°C, which corresponds to the loss of five $CH_3OH$ molecules and one $H_2O$ molecule (theoretical 4.88%). Then, the weight loss is 8.62%, when the temperature continues to rise from

152 °C to 360 °C. This process corresponds to a loss of seven $CH_3OH$ molecules, two $H_2O$ molecules and one $CH_3CN$ molecule (theoretical value is 8.68%). When the temperature continues to rise above 360 °C, cluster **2** was decomposed as the temperature continued to rise (Figure S2b).

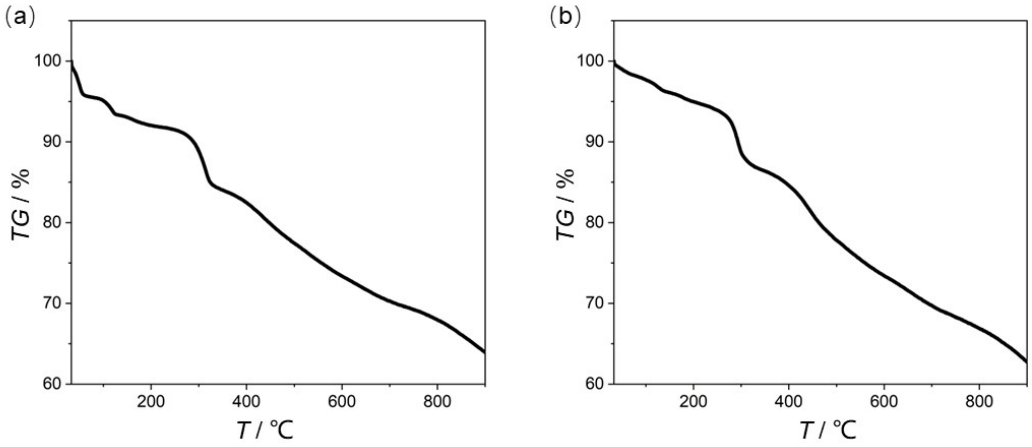


**Figure S2.** Thermogravimetric (TG) curves of clusters **1** and **2**.

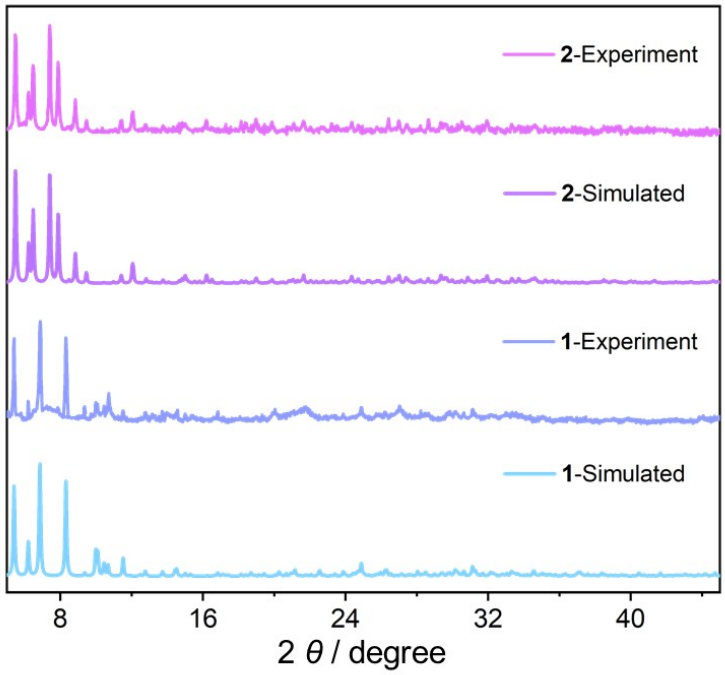


**Figure S3.** Powder X-ray diffraction patterns (PXRD) of clusters **1** and **2**.

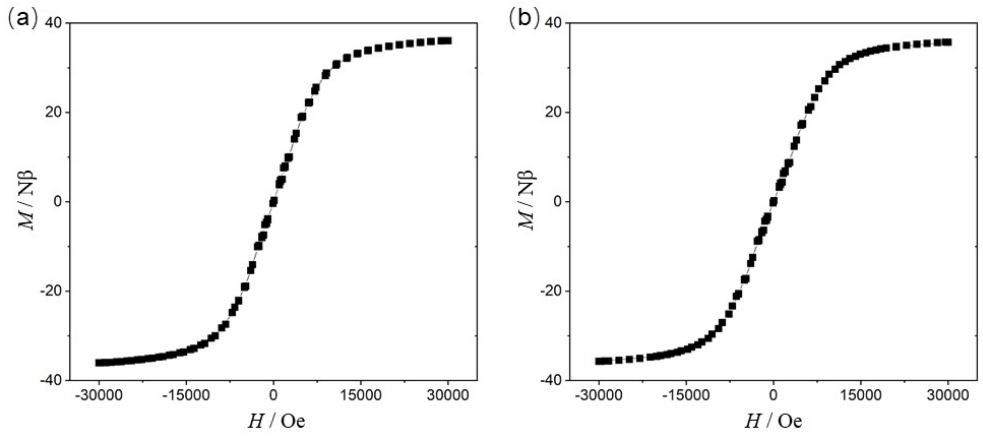


**Figure S4.** Loop curve graph of clusters **1** and **2** at 2 K.

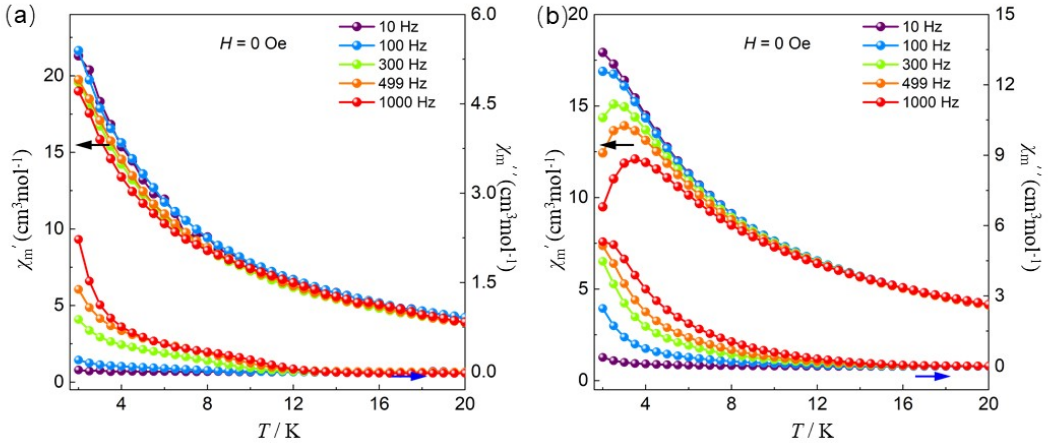


**Figure S5.** Temperature dependence of the real ($\chi'$) and imaginary ($\chi''$) ac susceptibilities at different frequencies in the 0 Oe dc fields for clusters **1** (a) and **2** (b).

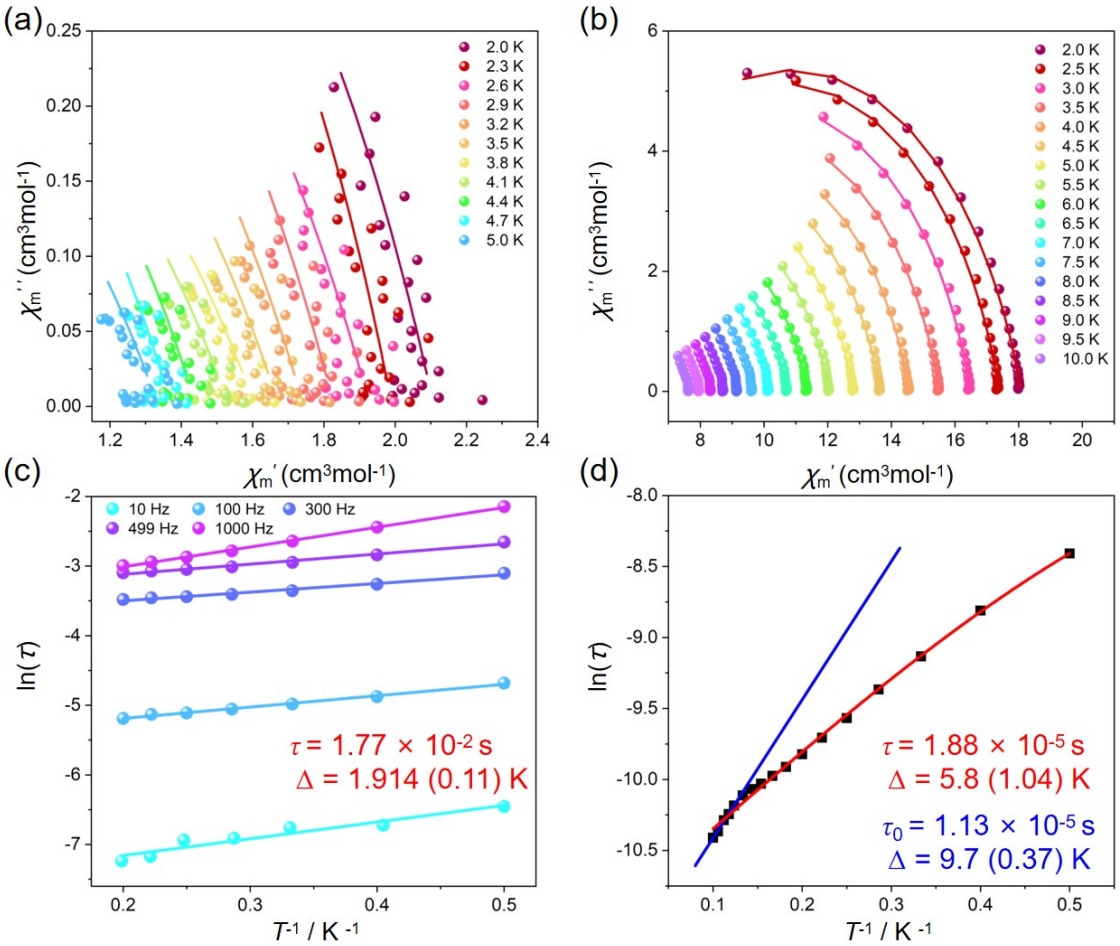


**Figure S6.** (a and b) Cole-Cole for clusters **1** and **2**; (c) Plots of ln($\chi''/\chi'$) *vs.* $T^{-1}$ for **1**; (d) Energy barrier fits for cluster **2**.

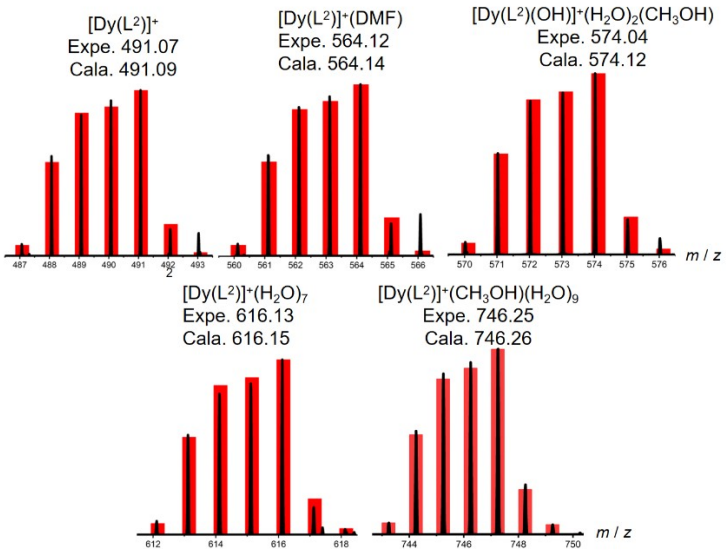

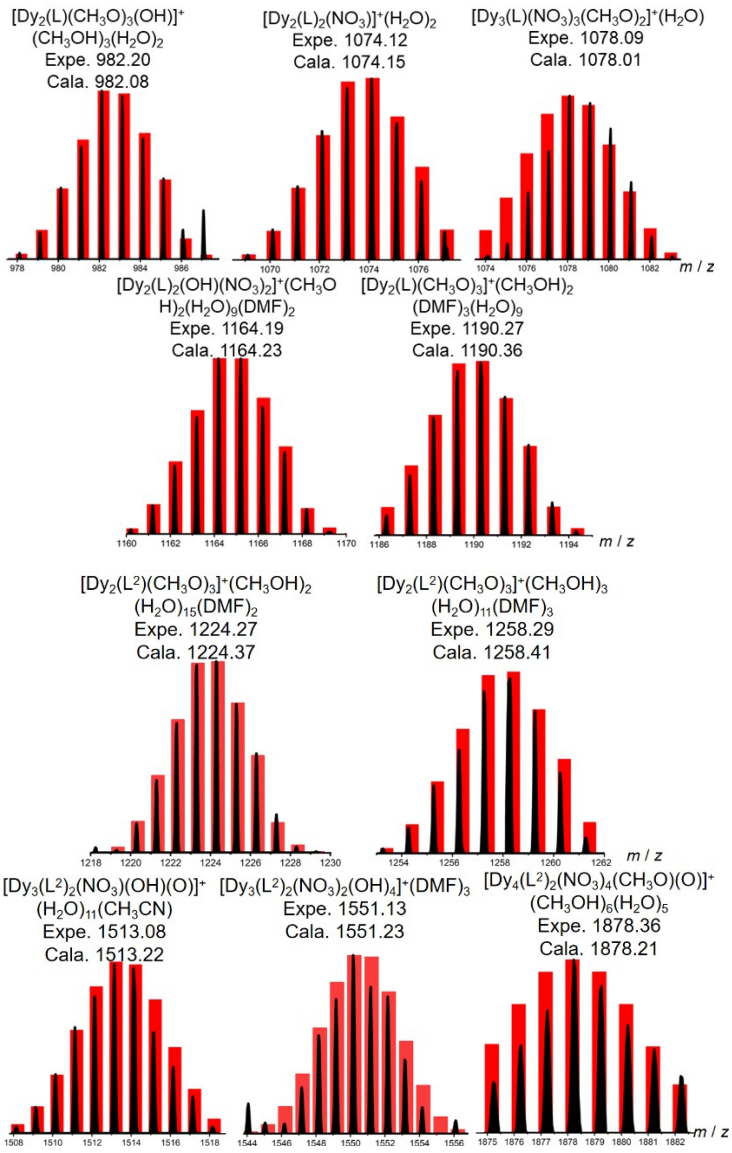


**Figure S7.** The fitting comparison of experimental and theoretical values of mass spectral molecular ion peaks of cluster **2**.

**Table S2.** Selected bond lengths (Å) and angles (°) of cluster **1** and **2**.

| **Bond lengths of complex 1 (Å)** | | | | | |
|---|---|---|---|---|---|
| Dy1-O5 | 2.250(6) | Dy2-O29$^{i}$ | 2.324(6) | Dy3-O68 | 2.479(6) |
| Dy1-O5$^{i}$ | 2.281(6) | Dy2-O43 | 2.348(6) | Dy3-O60 | 2.491(7) |
| Dy1-O54 | 2.339(6) | Dy2-O30 | 2.376(6) | Dy3-O57 | 2.554(7) |
| Dy1-O29 | 2.365(6) | Dy2-N40 | 2.436(7) | Dy4-O5 | 2.243(5) |
| Dy1-O43 | 2.406(6) | Dy3-O69 | 2.555(7) | Dy4-O19 | 2.246(6) |
| Dy1-O63 | 2.424(7) | Dy3-O61 | 2.276(6) | Dy4-O61 | 2.289(6) |

| | | | | | |
|---|---|---|---|---|---|
| Dy1-O32 | 2.451(6) | Dy3-O6 | 2.343(6) | Dy4-O54$^{i}$ | 2.309(6) |
| Dy1-O18 | 2.530(6) | Dy3-O55 | 2.366(6) | Dy4-O30 | 2.368(6) |
| Dy2-O44 | 2.249(6) | Dy3-O65 | 2.402(7) | Dy4-O18 | 2.423(6) |
| Dy2-O5 | 2.265(6) | Dy3-O30 | 2.425(6) | Dy4-N15 | 2.480(7) |
| Dy2-O6 | 2.314(6) | | | | |
| **Bond angles of complex 1 (°)** | | | | | |
| O5-Dy1-O5$^{i}$ | 75.7(2) | O6-Dy2-O43 | 84.5(2) | O55-Dy3-O57 | 126.7(2) |
| O5-Dy1-O54 | 124.8(2) | O29$^{i}$-Dy2-O43 | 103.5(2) | O6-Dy3-O69 | 140.1(2) |
| O5$^{i}$-Dy1-O54 | 72.4(2) | O44-Dy2-O30 | 81.2(2) | O55-Dy3-O69 | 73.1(2) |
| O5-Dy1-O29 | 119.5(2) | O5-Dy2-O30 | 76.2(2) | O65-Dy3-O69 | 67.8(2) |
| O5$^{i}$-Dy1-O29 | 73.1(2) | O6-Dy2-O30 | 71.0(2) | O30-Dy3-O69 | 127.8(2) |
| O54-Dy1-O29 | 92.5(2) | O29$^{i}$-Dy2-O30 | 96.8(2) | O68-Dy3-O69 | 51.2(2) |
| O5-Dy1-O43 | 70.8(2) | O6-Dy2-N40 | 101.0(2) | O60-Dy3-O69 | 68.3(2) |
| O5$^{i}$-Dy1-O43 | 98.6(2) | O29$^{i}$-Dy2-N40 | 91.1(2) | O57-Dy3-O69 | 102.0(2) |
| O54-Dy1-O43 | 70.9(2) | O43-Dy2-N40 | 65.1(2) | O6-Dy3-O55 | 79.7(2) |
| O29-Dy1-O43 | 163.2(2) | O30-Dy2-N40 | 154.5(2) | O65-Dy3-O57 | 134.8(2) |
| O5-Dy1-O63 | 146.3(2) | O5-Dy2-N40 | 129.2(2) | O30-Dy3-O57 | 130.3(2) |
| O5$^{i}$-Dy1-O63 | 137.8(2) | O61-Dy3-O6 | 86.0(2) | O68-Dy3-O57 | 68.3(2) |
| O54-Dy1-O63 | 78.8(2) | O61-Dy3-O55 | 147.3(2) | O60-Dy3-O57 | 50.9(2) |
| O29-Dy1-O63 | 78.1(2) | O43-Dy2-O30 | 135.1(2) | O61-Dy3-O69 | 131.5(2) |
| O43-Dy1-O63 | 100.4(2) | O44-Dy2-N40 | 74.1(2) | O30-Dy4-N15 | 154.4(2) |
| O5-Dy1-O32 | 80.4(2) | O5-Dy2-O43 | 71.6(2) | O18-Dy4-N15 | 64.4(2) |
| O5$^{i}$-Dy1-O32 | 156.2(2) | O61-Dy3-O65 | 80.9(2) | O5-Dy4-O19 | 153.8(2) |
| O54-Dy1-O32 | 123.1(2) | O6-Dy3-O65 | 143.6(2) | O5-Dy4-O61 | 105.8(2) |
| O29-Dy1-O32 | 120.1(2) | O55-Dy3-O65 | 93.6(2) | O19-Dy4-O61 | 86.2(2) |
| O43-Dy1-O32 | 73.2(2) | O6-Dy3-O30 | 69.7(2) | O5-Dy4-O54$^{i}$ | 73.6(2) |
| O63-Dy1-O32 | 66.0(2) | O55-Dy3-O30 | 75.2(2) | O19-Dy4-O54$^{i}$ | 90.1(2) |
| O5-Dy1-O18 | 68.6(2) | O65-Dy3-O30 | 74.1(2) | O61-Dy4-O54$^{i}$ | 169.2(2) |
| O5$^{i}$-Dy1-O18 | 100.31(19) | O61-Dy3-O68 | 85.1(2) | O5-Dy4-O30 | 76.8(2) |
| O54-Dy1-O18 | 160.3(2) | O6-Dy3-O68 | 140.1(2) | O19-Dy4-O30 | 85.0(2) |

| | | | | | |
|---|---|---|---|---|---|
| O29-Dy1-O18 | 67.82(19) | O55-Dy3-O68 | 124.0(2) | O61-Dy4-O30 | 73.2(2) |
| O43-Dy1-O18 | 128.76(19) | O65-Dy3-O68 | 72.4(2) | O54$^{i}$-Dy4-O30 | 96.3(2) |
| O63-Dy1-O18 | 96.5(2) | O30-Dy3-O68 | 142.0(2) | O5-Dy4-O18 | 70.7(2) |
| O32-Dy1-O18 | 70.5(2) | O61-Dy3-O60 | 125.4(2) | O19-Dy4-O18 | 134.6(2) |
| O44-Dy2-O5 | 152.6(2) | O6-Dy3-O60 | 79.0(2) | O61-Dy4-O18 | 84.1(2) |
| O44-Dy2-O6 | 87.1(2) | O55-Dy3-O60 | 80.5(2) | O54$^{i}$-Dy4-O18 | 105.6(2) |
| O5-Dy2-O6 | 100.0(2) | O65-Dy3-O60 | 135.5(2) | O30-Dy4-O18 | 133.1(2) |
| O44-Dy2-O29$^{i}$ | 93.4(2) | O30-Dy3-O60 | 143.0(2) | O5-Dy4-N15 | 128.5(2) |
| O5-Dy2-O29$^{i}$ | 74.2(2) | O68-Dy3-O60 | 75.0(2) | O19-Dy4-N15 | 72.1(2) |
| O6-Dy2-O29$^{i}$ | 167.6(2) | O61-Dy3-O57 | 74.6(2) | O61-Dy4-N15 | 93.6(2) |
| O44-Dy2-O43 | 135.8(2) | O6-Dy3-O57 | 71.9(2) | O54$^{i}$-Dy4-N15 | 95.0(2) |
| **Bond lengths of complex 2 (Å)** | | | | | |
| Dy1-O8$^{i}$ | 2.301(8) | Dy2-O3$^{i}$ | 2.290(8) | Dy3-O15 | 2.462(9) |
| Dy1-O8 | 2.246(9) | Dy2-O5 | 2.393(9) | Dy3-O11 | 2.349(8) |
| Dy1-O4 | 2.371(8) | Dy2-O7 | 2.359(9) | Dy3-O12 | 2.389(9) |
| Dy1-O10 | 2.491(8) | Dy2-N5 | 2.463(9) | Dy4-O8 | 2.271(8) |
| Dy1-O3 | 2.344(8) | Dy3-O20 | 2.557(9) | Dy4-O4$^{i}$ | 2.319(8) |
| Dy1-O5 | 2.498(8) | Dy3-O14 | 2.237(9) | Dy4-O1 | 2.257(9) |
| Dy1-O2 | 2.419(8) | Dy3-O7 | 2.426(8) | Dy4-O14 | 2.299(8) |
| Dy1-O9 | 2.401(9) | Dy3-O13 | 2.448(9) | Dy4-O7 | 2.401(9) |
| Dy2-O8 | 2.239(8) | Dy3-O18 | 2.494(9) | Dy4-O2 | 2.364(9) |
| Dy2-O11 | 2.298(8) | Dy3-O17 | 2.511(9) | Dy4-N2 | 2.455(10) |
| Dy2-O6 | 2.249(9) | | | | |
| **Bond angles of complex 2 (°)** | | | | | |
| O8-Dy1-O8$^{i}$ | 76.4(3) | O11-Dy2-O7 | 72.0(3) | O7-Dy3-O20 | 129.6(3) |
| O8-Dy1-O4 | 121.5(3) | O11-Dy2-N5 | 101.4(3) | O7-Dy3-O13 | 72.2(3) |
| O8$^{i}$-Dy1-O4 | 72.3(3) | O6-Dy2-O11 | 88.1(3) | O7-Dy3-O18 | 146.3(3) |
| O8-Dy1-O10 | 80.6(3) | O6-Dy2-O3$^{i}$ | 92.4(3) | O14-Dy3-O17 | 88.1(3) |
| O8$^{i}$-Dy1-O10 | 156.9(3) | O6-Dy2-O5 | 133.5(3) | O14-Dy3-O15 | 133.5(3) |
| O8-Dy1-O3 | 122.8(3) | O6-Dy2-O7 | 84.2(3) | O18-Dy3-O20 | 50.7(3) |

| | | | | | |
|---|---|---|---|---|---|
| O8$^{i}$-Dy1-O3 | 72.1(3) | O6-Dy2-N5 | 72.2(3) | O7-Dy3-O17 | 142.9(3) |
| O8-Dy1-O5 | 68.9(3) | O3$^{i}$-Dy2-O11 | 168.2(3) | O7-Dy3-O15 | 125.5(3) |
| O8$^{i}$-Dy1-O5 | 99.0(3) | O3$^{i}$-Dy2-O5 | 103.8(3) | O13-Dy3-O20 | 133.2(3) |
| O8$^{i}$-Dy1-O2 | 101.1(3) | O3$^{i}$-Dy2-O7 | 96.3(3) | O13-Dy3-O18 | 136.2(3) |
| O8-Dy1-O2 | 70.2(3) | O3$^{i}$-Dy2-N5 | 90.0(3) | O13-Dy3-O17 | 73.5(3) |
| O8$^{i}$-Dy1-O9 | 135.9(3) | O5-Dy2-N5 | 64.7(3) | O13-Dy3-O15 | 69.8(3) |
| O8-Dy1-O9 | 147.8(3) | O7-Dy2-O5 | 135.1(3) | O15-Dy3-O20 | 104.9(3) |
| O4-Dy1-O10 | 120.2(3) | O7-Dy2-N5 | 155.9(3) | O15-Dy3-O18 | 68.3(3) |
| O4-Dy1-O5 | 69.0(3) | O11-Dy3-O12 | 78.1(3) | O15-Dy3-O17 | 51.2(3) |
| O4-Dy1-O2 | 163.0(3) | O11-Dy3-O20 | 72.7(3) | O8-Dy4-O4$^{i}$ | 73.8(3) |
| O4-Dy1-O9 | 78.0(3) | O11-Dy3-O7 | 69.9(3) | O8-Dy4-O14 | 105.7(3) |
| O10-Dy1-O5 | 71.1(3) | O11-Dy3-O13 | 142.0(3) | O8-Dy4-O7 | 75.3(3) |
| O3-Dy1-O4 | 92.2(3) | O11-Dy3-O18 | 80.8(3) | O8-Dy4-O2 | 70.8(3) |
| O3-Dy1-O10 | 123.1(3) | O11-Dy3-O17 | 141.2(3) | O8-Dy4-N2 | 129.8(3) |
| O3-Dy1-O5 | 161.1(3) | O11-Dy3-O15 | 138.6(3) | O4$^{i}$-Dy4-O7 | 94.6(3) |
| O3-Dy1-O2 | 70.8(3) | O12-Dy3-O20 | 126.4(3) | O4$^{i}$-Dy4-O2 | 106.0(3) |
| O3-Dy1-O9 | 77.3(3) | O12-Dy3-O7 | 76.7(3) | O4$^{i}$-Dy4-N2 | 96.1(3) |
| O2-Dy1-O10 | 71.8(3) | O12-Dy3-O13 | 96.7(3) | O1-Dy4-O8 | 150.7(3) |
| O2-Dy1-O5 | 128.0(3) | O12-Dy3-O18 | 81.3(3) | O1-Dy4-O4$^{i}$ | 87.5(3) |
| O9-Dy1-O10 | 67.2(3) | O12-Dy3-O17 | 121.2(3) | O1-Dy4-O14 | 86.7(3) |
| O9-Dy1-O5 | 99.9(3) | O12-Dy3-O15 | 70.7(3) | O1-Dy4-O7 | 84.2(3) |
| O9-Dy1-O2 | 97.9(3) | O14-Dy3-O11 | 86.5(3) | O1-Dy4-O2 | 137.4(3) |
| O8-Dy2-O11 | 100.8(3) | O14-Dy3-O12 | 148.1(3) | O1-Dy4-N2 | 73.5(3) |
| O8-Dy2-O6 | 155.1(3) | O14-Dy3-O20 | 73.4(3) | O14-Dy4-O4$^{i}$ | 165.1(3) |
| O8-Dy2-O3$^{i}$ | 74.2(3) | O14-Dy3-O7 | 71.8(3) | O14-Dy4-O7 | 71.2(3) |
| O8-Dy2-O5 | 70.9(3) | O14-Dy3-O13 | 78.5(3) | O14-Dy4-O2 | 87.5(3) |
| O8-Dy2-O7 | 76.7(3) | O14-Dy3-O18 | 123.9(3) | O14-Dy4-N2 | 95.4(3) |
| O8-Dy2-N5 | 127.3(3) | O18-Dy3-O17 | 70.7(3) | O7-Dy4-N2 | 154.7(3) |
| O11-Dy2-O5 | 84.3(3) | O17-Dy3-O20 | 68.9(3) | O2-Dy4-O7 | 132.9(3) |
| O2-Dy4-N2 | 65.1(3) | | | | |

**Table S3**. *SHAPE* analysis of the Dy1 in the clusters **1** and **2**.

| Label | Shape | Symmetry | Distortion (°) | |
|---|---|---|---|---|
| | | | Dy1 (1) | Dy1 (2) |
| HP-7 | $D_{7h}$ | Heptagon | 47.67678 | 46.41484 |
| HPY-7 | $C_{6v}$ | Hexagonal pyramid | 35.02654 | 33.98077 |
| PBPY-7 | $D_{5h}$ | Pentagonal bipyramid | 27.14682 | 27.20226 |
| COC-7 | $C_{3v}$ | Capped octahedron | 28.55928 | 28.25368 |
| CTPR-7 | $C_{2v}$ | Capped trigonal prism | 27.44894 | 27.95044 |
| JPBPY-7 | $D_{5h}$ | Johnson pentagonal bipyramid J13 | 32.28464 | 32.37441 |
| JETPY-7 | $C_{3v}$ | Johnson elongated triangular pyramid J7 | 33.75690 | 32.91938 |

**Table S4**. *SHAPE* analysis of the Dy2 in the clusters **1** and **2**.

| Label | Shape | Symmetry | Distortion (°) | |
|---|---|---|---|---|
| | | | Dy2 (1) | Dy2 (2) |
| OP-8 | $D_{8h}$ | Octagon | 44.71560 | 44.57769 |
| HPY-8 | $C_{7v}$ | Heptagonal pyramid | 31.60690 | 31.41839 |
| HBPY-8 | $D_{6h}$ | Hexagonal bipyramid | 29.64515 | 29.54543 |
| CU-8 | $O_h$ | Cube | 24.95490 | 24.79237 |
| SAPR-8 | $D_{4d}$ | Square antiprism | 25.30011 | 25.31050 |
| TDD-8 | $D_{2d}$ | Triangular dodecahedron | 23.11296 | 23.23515 |
| JGBF-8 | $D_{2d}$ | Johnson gyrobifastigium J26 | 30.31710 | 30.66463 |
| JETBPY-8 | $D_{3h}$ | Johnson elongated triangular bipyramid J14 | 37.59994 | 37.49979 |
| JBTP-8 | $C_{2v}$ | Biaugmented trigonal prism J50 | 25.08216 | 25.26054 |
| BTPR-8 | $C_{2v}$ | Biaugmented trigonal prism | 25.40354 | 25.90108 |
| JSD-8 | $D_{2d}$ | Snub dipHenoid J84 | 26.10376 | 26.33839 |
| TT-8 | $T_d$ | Triakis tetrahedron | 23.56992 | 23.44739 |
| ETBPY-8 | $D_{3h}$ | Elongated trigonal bipyramid | 35.36388 | 36.02676 |

**Table S5**. *SHAPE* analysis of the Dy3 in the clusters **1** and **2**.

| Label | Shape | Symmetry | Distortion (°) | |
|---|---|---|---|---|
| | | | Dy3 (1) | Dy3 (2) |
| HP-7 | $D_{7h}$ | Heptagon | 46.43467 | 47.09985 |
| HPY-7 | $C_{6v}$ | Hexagonal pyramid | 34.34694 | 35.58078 |
| PBPY-7 | $D_{5h}$ | Pentagonal bipyramid | 27.37341 | 27.31557 |
| COC-7 | $C_{3v}$ | Capped octahedron | 28.59610 | 28.78542 |
| CTPR-7 | $C_{2v}$ | Capped trigonal prism | 28.16606 | 27.69416 |
| JPBPY-7 | $D_{5h}$ | Johnson pentagonal bipyramid J13 | 32.70556 | 32.44131 |
| JETPY-7 | $C_{3v}$ | Johnson elongated triangular pyramid J7 | 32.92396 | 33.76365 |

**Table S6**. *SHAPE* analysis of the Dy4 in the clusters **1** and **2**.

| Label | Shape | Symmetry | Distortion (°) | |
|---|---|---|---|---|
| | | | Dy4 (1) | Dy4 (2) |
| EP-9 | $D_{9h}$ | Enneagon | 48.25672 | 43.71009 |
| OPY-9 | $C_{8v}$ | Octagonal pyramid | 38.01793 | 35.61322 |
| HBPY-9 | $D_{7h}$ | Heptagonal bipyramid | 35.17871 | 34.06055 |
| JTC-9 | $C_{3v}$ | Johnson triangular cupola J3 | 28.54213 | 23.81293 |
| JCCU-9 | $C_{4v}$ | Capped cube J8 | 28.92568 | 27.21980 |
| CCU-9 | $C_{4v}$ | Spherical-relaxed capped cube | 28.33736 | 27.78523 |
| JCSAPR-9 | $C_{4v}$ | Capped square antiprism J10 | 22.56189 | 21.20988 |
| CSAPR-9 | $C_{4v}$ | Spherical capped square antiprism | 22.46010 | 21.64890 |
| JTCTPR-9 | $D_{3h}$ | Tricapped trigonal prism J51 | 21.11212 | 20.46027 |
| TCTPR-9 | $D_{3h}$ | Spherical tricapped trigonal prism | 22.51160 | 21.90571 |
| JTDIC-9 | $C_{3v}$ | Tridiminished icosahedron J63 | 31.54964 | 28.27652 |
| HH-9 | $C_{2v}$ | Hula-hoop | 28.88224 | 28.13913 |
| MFF-9 | $C_s$ | Muffin | 22.12765 | 22.03713 |

**Table S7.** Parameters from the fitting result of the Cole-Cole plots for the cluster **1** under 0 Oe field.

| | **1** | | |
|---|---|---|---|
| *T*emp.(K) | $\tau$ | $\alpha$ | residual |
| 2.0 | 6.42814E-6 | 0.463 | 0.0666 |
| 2.3 | 5.84223E-6 | 0.42326 | 0.05574 |
| 2.6 | 2.52193E-6 | 0.53267 | 0.06066 |
| 2.9 | 2.47095E-6 | 0.51236 | 0.04936 |
| 3.2 | 1.63708E-6 | 0.55178 | 0.0461 |
| 3.5 | 1.03053E-6 | 0.59284 | 0.05261 |
| 3.8 | 6.48952E-7 | 0.62752 | 0.04035 |
| 4.1 | 7.12875E-7 | 0.6206 | 0.04059 |
| 4.4 | 9.72806E-7 | 0.57349 | 0.03696 |
| 4.7 | 1.03708E-6 | 0.55546 | 0.02877 |
| 5.0 | 6.21776E-7 | 0.61446 | 0.03936 |

**Table S8.** Parameters from the fitting result of the Cole-Cole plots for the cluster **2** under 0 Oe field.

| | **2** | | |
|---|---|---|---|
| *T*emp.(K) | $\tau$ | $\alpha$ | residual |
| 2 | 2.23008E-4 | 0.18964 | 0.10006 |
| 2.5 | 1.49185E-4 | 0.17692 | 0.07606 |
| 3 | 1.08023E-4 | 0.17657 | 0.06318 |
| 3.5 | 8.56003E-5 | 0.17877 | 0.04731 |
| 4 | 6.99515E-5 | 0.1855 | 0.03796 |

| | | | |
|---|---|---|---|
| 4.5 | 6.09243E-5 | 0.18915 | 0.03041 |
| 5 | 5.42331E-5 | 0.19344 | 0.0261 |
| 5.5 | 4.96142E-5 | 0.19695 | 0.02171 |
| 6 | 4.65577E-5 | 0.19849 | 0.02018 |
| 6.5 | 4.40635E-5 | 0.20072 | 0.01459 |
| 7 | 4.2437E-5 | 0.19874 | 0.01541 |
| 7.5 | 4.05654E-5 | 0.20079 | 0.01131 |
| 8 | 3.66212E-5 | 0.20715 | 0.00891 |
| 8.5 | 3.55635E-5 | 0.20384 | 0.00888 |
| 9 | 3.37898E-5 | 0.20399 | 0.00797 |
| 9.5 | 3.32683E-5 | 0.19693 | 0.00737 |
| 10 | 3.01148E-5 | 0.1952 | 0.00602 |

**Table S9**. Selected parameters from the fitting result of the Cole-Cole plots for **1** under 0 Oe fields.

| Frequency (Hz) | $\boldsymbol{\Delta}$ (K) | $\boldsymbol{\tau_0}$ (s) |
|---|---|---|
| 10 | 2.84788 | $2.78\times10^{-2}$ |
| 100 | 1.45621 | $3.33\times10^{-2}$ |
| 300 | 1.24737 | $2.35\times10^{-2}$ |
| 499 | 1.63634 | $4.02\times10^{-3}$ |
| 100 | 2.40405 | $4.80\times10^{-4}$ |